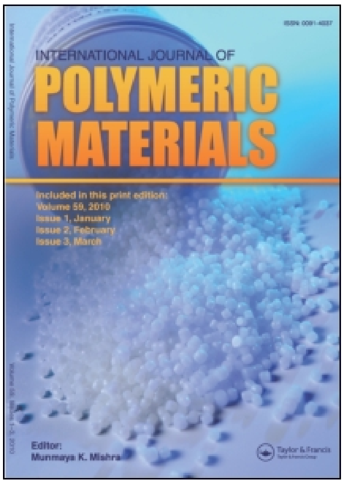

International Journal of Polymeric Materials
Publication details, including instructions for authors and subscription information:
http://www.informaworld.com/smpp/title~content=t713647664

The Conductivity Distribution in Injection Moulded LDPE and HDPE Filled with Carbon Black

Carl Klason[a]; Josef Kubát[a]
[a] Department of Polymeric Materials, Chalmers University of Technology, Gothenburg, Sweden

To cite this Article Klason, Carl and Kubát, Josef(1984) 'The Conductivity Distribution in Injection Moulded LDPE and HDPE Filled with Carbon Black', International Journal of Polymeric Materials, 10: 4, 259 — 280
To link to this Article: DOI: 10.1080/00914038408078645
URL: http://dx.doi.org/10.1080/00914038408078645

Intern. J. Polymeric Mater., 1984, Vol. 10, pp. 259–280
0091–4037/84/1004–0259 $18.50/0

Printed in the United Kingdom

The Conductivity Distribution in Injection Moulded LDPE and HDPE Filled with Carbon Black

CARL KLASON and JOSEF KUBÁT

Chalmers University of Technology, Department of Polymeric Materials,
S-412 96 Gothenburg, Sweden

This study of the distribution of conductivity in injection-moulded compositions (test bars) of LDPE and HDPE containing carbon black (20% Vulcan XC-72, 10% Ketjenblack EC) showed that the skin and shear zones have substantially higher resistivity levels than the core. In general, the resistivity increased with the degree of orientation, as determined by thermal shrinkage measurements. There was, however, no simple relation between resistivity and shrinkage. Regions with increased resistivity showed a pronounced frequency dependence, the resistivity decreasing with increasing frequency; in annealed samples or samples taken from the core, the resistivity was frequency independent. Annealing restored the high conductivity of isotropic samples. The results are in qualitative agreement with the assumption of a conducting CB-network changing its connectivity upon deformation and flow, and recovering when the sample is annealed.

INTRODUCTION

Within certain temperature ranges, polymers containing conductive fillers often show positive values of the temperature coefficient of resistivity.[1–6] This effect, which is known as the PTC-effect, has been interpreted as resulting from the disruption of the conductive network due to the melting of the polymer. Upon cooling, the network is reformed, restoring the original resistivity level.[1–3,7] Commercial applications in self-limiting heaters and similar devices, where crystalline polymers filled with carbon black (CB) are normally used, have been reported.[8,9]

The resistivity and the PTC-effect in crystalline polymers containing carbon black have been studied with regard to their dependence on the filler type and concentration,[2,10–12] polymer type,[1–5,13–15] cross-linking,[16,17] and heat-treatment.[18] Not properly accounted for, however, is the role of processing and the resulting orientation distribution.

This paper presents the results of an experimental study of the variation of the resistivity with the orientation within injection-moulded test bars. The materials used were low-density and high-density polyethylene (LDPE, HDPE) containing two grades of carbon black at 10% and 20% filling level, respectively. It will be shown that the variation in conductivity in different parts of the sample (distance from the surface) is appreciable, amounting to 6–8 decades between the surface and the core. In general, the resistivity increases with orientation. The data are supplemented by orientation values at varying distance from the surface, measured as thermal shrinkage. Among the effects observed was a pronounced frequency dependence (DC to 10 kHz) of the resistivity for samples (microtome cuttings) having the highest resistivity (surface). In such samples, there was an inverse relationship between resistivity and frequency. In the core of the moulded test bars no frequency dependence was recorded. The corresponding PTC-data will be presented in a forthcoming paper.

Available data on the influence of mechanical deformation (orientation) on the resistivity parameters appear to have been measured mainly on CB-filled elastomers. The variation of the resistivity, ρ, may be understood qualitatively in terms of an independent CB-network in the elastomer matrix. At relatively small deformations, the network is disrupted, and the ρ-value increases (Mullins effect). Further increase in deformation produces an alignment of the CB-chains with a decrease in ρ as result. At still larger deformations, the coupling between the CB-particles and the polymer chains is destroyed and ρ starts to rise again.[19–21] The change in ρ at different stages of deformation depends strongly on the type and concentration of the conductive filler, elastomer type, and compounding method. Results obtained by different authors may thus appear contradictory.[19]

Compounds at the higher conductivity end show a relatively small dependence on deformation. According to Ref. 21, ρ of an SBR/15 pph Ketjen EC remained practically constant to 150% extension. In moderately conducting systems, ρ increased *c.* 2 decades at 50% extension. Similar values are found in Ref. 22, together with results showing that also the ρ-value in the transversal direction increases upon deformation (*c.* 4.5 decades at 50% strain). The variability of the results is illustrated by the variation of $\rho_{\perp}/\rho_{\|}$, which has a maximum for SBR/20% CB, while the corresponding NR-compound shows no such effect.[22]

The time-dependent reformation of the CB-network after an initial disruption is treated in[23,24] for the case of shear stress relaxation. Again, the results are highly sensitive to the CB-structure, concentration, vulcanization conditions, etc. They also show the basic similarity between shear and extensional strains. In samples deformed and subsequently unloaded, ρ falls slowly with time, following the initial increase.[25,26] In certain cases,[27] the unloading may result in a further increase in ρ, before the recovery process sets in.

In dynamic tests, ρ tends to remain constant at small amplitudes; larger amplitudes raise the ρ-level.[28-30] The in-phase shear modulus and the conductivity were found to vary in an approximately similar way when the amplitude was increased.[31] Also in dynamic tests, the results depend heavily on the compounding parameters.[32]

Hydrostatic compression[33-35] normally produces a decrease in ρ. Similar effects in uniaxial compression are utilized in switches.[36]

Unlike that of CB-based compounds, the ρ-level of elastomeric TNCQ-complexes remained constant or decreased somewhat with elongation (*c.* 50% at 80% elongation). The reproducibility was far better than that normally found with CB-filled rubbers.[37]

The conductivity of injection-moulded and extruded samples of CB-containing thermoplastics (HDPE, PP, PVC, EVA) is reported in Refs. 38 and 39. In all cases was the resistivity substantially higher than in the corresponding compression-moulded samples (by 1 to 6 decades). A pronounced anisotropy of the conductivity was also recorded. In some cases the ρ-value was higher in the longitudinal direction; in others the opposite was true. The results have, however, not been analysed in detail. Also in blown films of CB-filled PE the resistivity increased with the degree of orientation, and an anisotropic behaviour of ρ developed.[40] In PE/polyisobutylene/CB mixtures,[41] higher extrusion rates resulted in an increase of ρ. The effect of extrusion variables is also treated in Refs. 42 and 43; the longitudinal ρ-value was reduced by drawing down the extrudate when leaving the die.

In the book by Norman[44] the reader may find further references on the influence of processing on the electrical parameters, mainly with regard to conductive rubbers. For thermoplastics, the information is scarce and qualitative only, which is also the case in the literature published after the appearance of Ref. 44.

EXPERIMENTAL

Materials

Two electrically conducting CB-types were used as fillers in LDPE and HDPE; the physical characteristics are given in Table I. One of the CB-grades, Ketjenblack EC, is especially efficient in producing a high conductivity at low loading levels (leaf-like, very porous structure). The other CB-grade, Vulcan XC-72, is also of the electrical conduction type, but requires twice as high loadings as Ketjenblack

TABLE I

Materials used

Carbon black	Ketjenblack EC (AKZO)	Vulcan XC-72 (Cabot)
BET surface area, m^2/g	930	254
DBP absorption ml/100 g	350	178
Volatiles, %	1.0	1.5
Particle diameter, millimicron	30	30
Polymer	**LDPE (ICI, 017.040)**	**HDPE (Unifos, DMDS 2215)**
Density kg/m^3	917	953
Melt flow index (MFI 190/2.16) g/10 min	7	0.1

EC to give a resistivity (ρ) in the range of 10^2–10^5 Ωcm. A detailed description of the two carbon black types is given in Ref. 21.

The CB-concentration used was 10% with Ketjenblack (KBEC) and 20% with Vulcan XC-72 (VXC) in order get a resistivity level of *c.* 10^3 Ωcm for both LDPE and HDPE. Because of the steepness of the ρ-concentration curve for KBEC, reproducible values were difficult to obtain at concentrations below 10%.

The resistivity vs. concentration of CB is shown in Figure 1. The KBEC-grade produces a conductive network at lower concentration than VXC.[21] Furthermore, the curve for KBEC is steep up to *c.* 10%, whereafter increasing the concentration produces a marginal

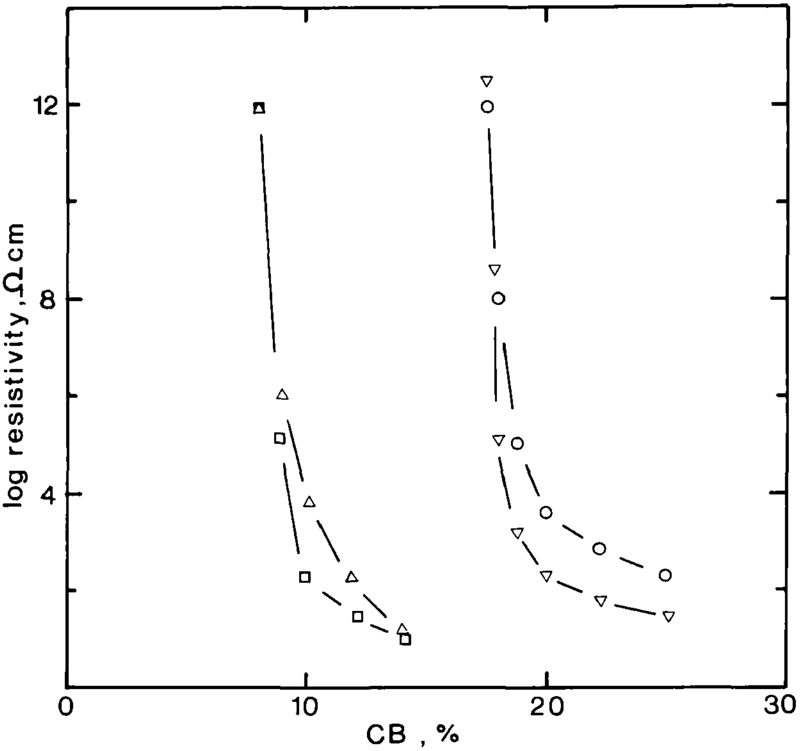

FIGURE 1 Resistivity vs. concentration of carbon black. Compression moulded samples (200°C, heating without pressure for 15 min, 30 MPa for 2 min, cooling 5°C/min). △ = LDPE/KBEC, ○ = LDPE/VXC, □ = HDPE/KBEC, ▽ = HDPE/VXC.

decrease in ρ only. For VXC, the decrease in ρ is continuous. The shape of the curves is in accordance with available data.[21]

The behaviour of LDPE and HDPE is largely similar. However, the ρ-level of HDPE is lower than that of LDPE at similar CB-loadings, supporting the idea that CB is mainly dispersed in the amorphous regions.[1]

Mixing and injection moulding

The polymer/CB-compounds were mixed using a Buss–Kneader (mixing extruder) with a vented screw (Type PR 46, D = 46 mm, L = 11 D). To achieve a reproducible resistivity level the mixing operation had to be repeated twice. The residence time in the Buss machine was *c.* 2 min. The extrudate was hot-pelletized and dried at 100°C for 24 h before injection moulding.

With regard to the ρ-value, the KBEC-based compounds were relatively insensitive to processing conditions, as repeated mixing, injection moulding, remixing, granulating, and another injection moulding. During such operations, the ρ-value remained constant within 30%. For VXC, an increase in ρ of 30–100% was noted when the compound was treated according to the above scheme. These changes are to be considered small; they are explained in terms of the higher structure of VXC resulting from prolonged mechanical treatment.[21]

The injection moulding was performed on a conventional machine

TABLE II

Injection moulding conditions

Polymer compound	Melt temperature °C	Mould temperature °C	Injection pressure MPa	Packing pressure MPa	Injection speed	Degree of orientation
LDPE/10% KBEC	200	25	110	70	High	Normal
LDPE/10% KBEC	160	25	110	100	Slow	High
LDPE/20% VXC	200	25	110	70	High	Normal
LDPE/20% VXC	160	25	110	100	Slow	High
HDPE/10% KBEC	280	75	110	80	High	Normal
HDPE/10% KBEC	200	25	110	100	High	High
HDPE/20% VXC	280	75	110	80	High	Normal
HDPE/20% VXC	200	25	110	100	High	High

(Arburg 221 E/170 R). Apart from normal moulding conditions, the settings of the machine were chosen to give a high degree of orientation in the samples (DIN tensile strength test bar, area 10×3.5 mm, effective length 75 mm), i.e. a low melt temperature and a cooled mould. Using a slow injection speed also increased the degree of orientation (cf. Table II).

Determination of orientation and internal stresses

As a measure of the orientation in different layers of the injection-moulded samples, the shrinkage of thin slices (thickness 30 μm) cut with a microtome (Leitz, type 1400) was used. The lateral dimensions of the slices (length 15 mm, width 4.0 mm) were determined before and after heat treatment in a silicone bath for 10 min at 120 and 130°C for LDPE and HDPE, respectively. The shrinkage values were corrected for lateral effects.[45] The result were in good agreement with those found by other authors[45,46]. The S_L and S_T values (longitudinal and transversal shrinkage) given below are average values of five single determinations. Shrinkage measurements on whole test bars did not produce any useful results (warpage etc.).

The internal stress aspect has been considered for the sake of completeness only, as the electrical parameters did not correlate with internal stress data. Internal stresses were introduced by quenching from 140 to 0°C. The resistivity of the LDPE-samples increased about 50% (scatter 30%). Compared with the effect of varying orientation, the influence of stress introduced in this way was small. The internal stress level in the quenched samples was not measured.

Measurement of resistivity

The bulk and surface resistivity, ρ_B and ρ_s, were measured using conventional techniques with both DC (Keithley Electrometer Model 160 B, applied voltage 1 V, above 10^{10} Ωcm increasing to 100 volt) and AC (50 Hz–10^4 Hz, General Radio Conductance Bridge Type 1630, applied voltage 1.0 V). The ρ-values were determined in both the flow direction (length axis of the tensile testing bars) and the two cross-directions perpendicular to it. A rectangular coordinate system (x, y, z) was introduced as shown in Figure 3.

The bulk resistivity, ρ_B, was determined according to method A and B and the surface resistivity, ρ_s, according to method C, specified as follows:

Bulk resistivity

A. On a middle part (10 × 10 × 3.5 mm) cut from the test bar. In this way the overall resistivity was determined in the *x*, *y*, and *z*-directions.
B. On the individual cuts (60 μm).

Surface resistivity

C. On the remaining surface of the sample after removal of a given number of layers (30 μm) with the microtome; ρ_s was determined (modified ASTM D 257) using two 1 × 1 × 10 mm electrodes placed 1 mm apart. The ρ_s-value was measured in the *x*- and *y*-directions only.

Method C gives mainly ρ_s, although the bulk material may have a certain influence.

RESULTS

Orientation (shrinkage)

The orientation pattern divides an injection-moulded part into three layers: skin, shear zone, and core. The orientation of the skin is due to the biaxial stretching of the moving melt front, while that of the shear zone is caused by a uniaxial shear field acting in the flow direction. The core region normally shows the structure of the polymer solidified at rest, as effects induced by the shear field are relaxed due to longer cooling times. The orientation pattern is the result of an interplay between the elongational (skin) and shear flow field (shear zone), and the temperature distribution across the part during the cooling stage. The internal stress distribution is, however, associated with the latter factor only.

Two types of samples with different overall orientations were produced by adjusting the moulding conditions as described above. The shrinkage data for the two types of test bars given in Figure 2 are in agreement with the orientation patterns known from the literature.[45]

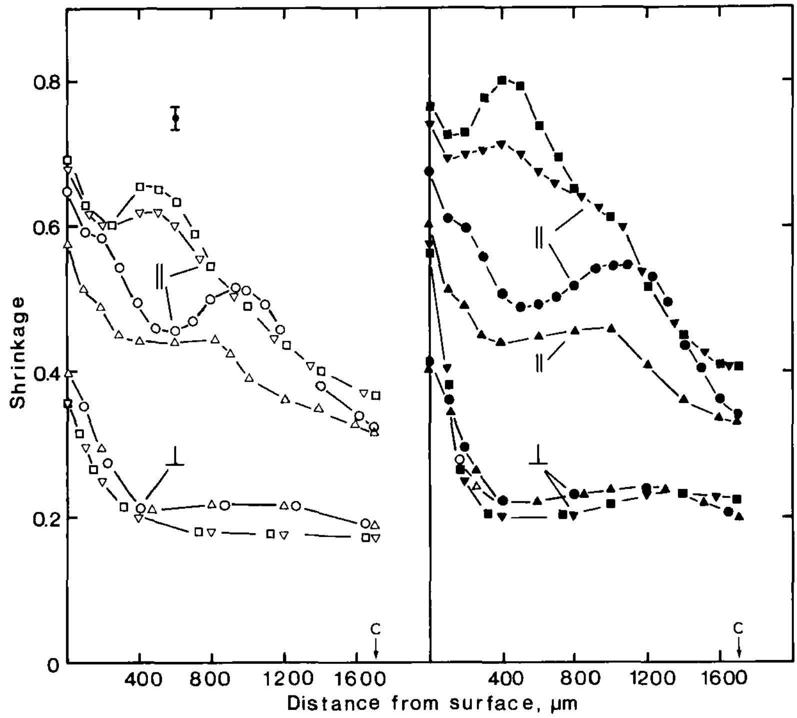

FIGURE 2 Longitudinal (||) and transversal (⊥) shrinkage values vs. distance from surface of injection moulded test bars. Symbols: LDPE with 10% KBEC (△), LDPE with 20% VXC (○), HDPE with 10% KBEC (□), HDPE with 20% VXC (▽); open symbols, normal orientation (left); filled symbols, high orientation (right).

For LDPE, the surface layer (skin) is highly oriented, even in the transverse direction, the deeper lying layers being oriented mainly in the flow direction. The shear zone is not as clearly developed as for HDPE; it is visible as an inflexion only for the highly oriented sample. Such samples show a higher degree of orientation in the longitudinal direction, while in the transverse direction the influence of processing conditions is negligible. The second peak at about 1 mm from the surface, clearly visible for LDPE, is likely to be due to the flow of the material during the packing state.[47] The influence of the CB-type and loading (10% KBEC, 20% VXC) on the orientation distribution was not significant.

The shrinkage vs. distance from the surface for HDPE-samples containing 10% (KBEC) and 20% (VXC) is also shown in Figure 2.

The difference in orientation between the two directions is substantially higher than for LDPE. There is a slight difference between the two CB-types, KBEC producing a slightly higher longitudinal orientation. The shear zone peak appears to be more developed than for LDPE, while the opposite applies to the packing peak.

The higher orientation obtained with HDPE may be related to the relatively high molecular weight of the polymer used (low melt flow index) and a low dependence of its viscosity on temperature.

The orientation levels in the longitudinal direction may be classified as relatively high, with changes in the processing conditions producing only minor effects.

Resistivity

Overall bulk resistivity Figure 3 shows the frequency dependence of ρ_B of the test bar with a normal orientation, measured in the three principal directions for LDPE and HDPE, both with 10% KBEC and 20% VXC. The lowest ρ-values were obtained in the x-direction for both types of PE. While for HDPE the difference between this direction and the two others was relatively small, it was several orders of magnitude for LDPE. It should also be noted that the higher the resistivity, the higher was its frequency (f) dependence, the ρ-values decreasing with increasing f. For the highest ρ-values, this decrease amounted to several decades in the range of DC–10 kHz.

With regard to the influence of the CB-type, KBEC gave a higher resistivity level with LDPE, which is significant especially in the z-direction. With HDPE, no difference between KBEC and VXC was found.

The ρ-levels do not correlate in any simple way with the orientation in Figure 2. For instance, the orientation of the HDPE-sample was higher than that of LDPE. This is not reflected in the ρ-values shown in Figure 3.

The result relating to the samples with the higher orientation are reproduced in Figure 4. For HDPE, the difference between the x-direction and the other directions was here substantially higher. Again the x-directions had the lowest resistivity. The ρ-levels in the y- and z-directions were well separated. The greatest influence of

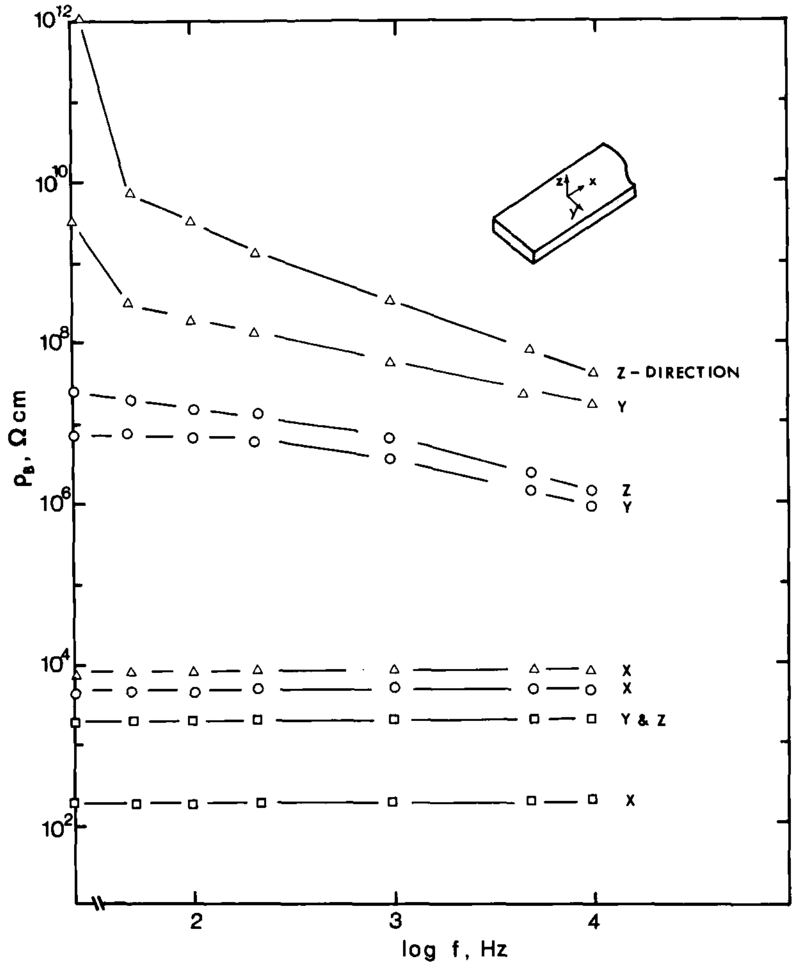

FIGURE 3 Frequency dependence of overall bulk resistivity, ρ_B, of the test bar with a normal orientation, measured in the three principal directions (*x*, *y* and *z*). Symbols as in Figure 2.

orientation on ρ was also in this case found for LDPE. KBEC gave a slightly higher resistivity than VXC. There was practically no DC-conductivity in the transverse directions for LDPE with 10% KBEC or 20% VXC ($\rho = 10^{11} - 10^{12}$ Ωcm). The frequency dependence of ρ was similar to that shown in Figure 3.

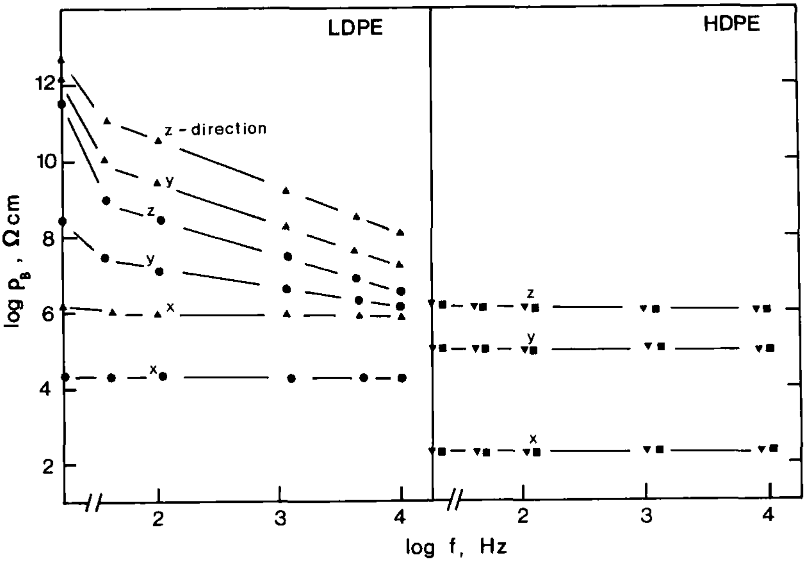

FIGURE 4 Frequency dependence of overall bulk resistivity of the test bar with a high orientation, measured in the three principal directions. Symbols as in Figure 2.

Changes in the ρ-level induced by the higher orientation of these samples are much larger than the changes reflected in the corresponding shrinkage data.

Bulk resistivity–microtome cuttings The distribution of orientation in injection-moulded samples calls for measurements of the bulk resistivity on thin slices taken at varying distance from the surface. However, the reliability of such measurements suffers from the inevitable damage imparted to the thin cuttings (60 μm) by the microtome knife. These values should therefore be considered with caution.

The bulk resistivity of such cuttings has been measured on HDPE only. For LDPE, the bulk resistivity was practically the same as the corresponding surface value (see below).

The ρ-values for HDPE with 10% KBEC shown in Figure 5 are unusually high when compared to the data in Figure 3 and 4, indicating possible damage during cutting.

The dependence of the resistivity on the distance from the surface is clearly seen from the data of Fig. 5. The variation of ρ_B with the

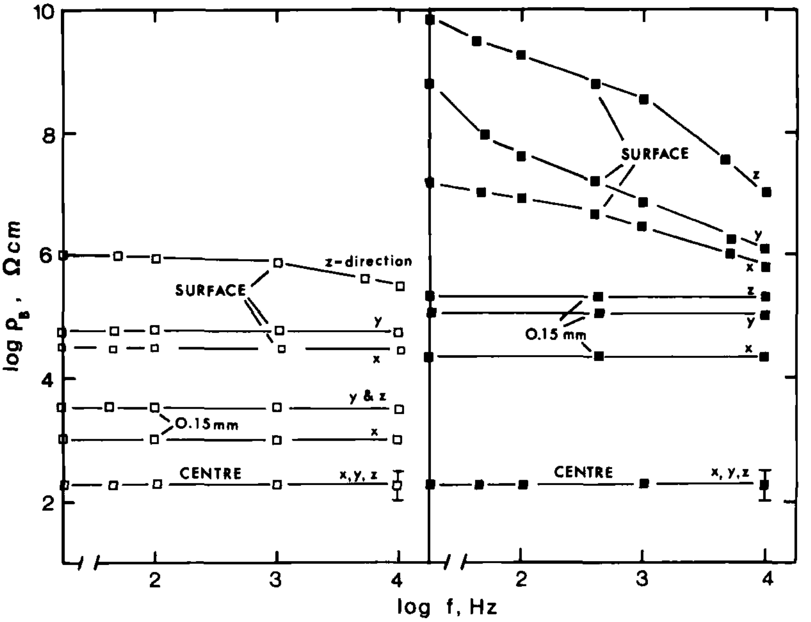

FIGURE 5 Frequency dependence of the bulk resistivity, ρ_B, of microtome cuttings (thickness 60 μm) at the surface, and 0.15 mm and 1.7 mm (centre) from the surface. HDPE with 10% KBEC; open symbols, normal orientation (left); filled symbols, high orientation (right).

direction was basically similar to that revealed by the data shown above. At the surface, the difference between the x-direction and the other two directions was the largest; it decreased towards the centre of the sample, where ρ_B has the same value for all three directions. At the same time, the overall ρ_B-level decreased markedly from the surface towards the centre, the decrease being 6–8 decades, depending on the direction. Interesting is also the diminishing difference between the y- and z-directions as one moves from the surface. With regard to the effect of frequency on the ρ_B-value, this dependence decreased with the ρ-level. Below *c.* 10^6 Ωcm, the ρ-values were independent of f.

For the sample with the higher orientation the ρ-values were higher (cf. Figs 3 and 4), except at the centre, where the ρ-level was independent of the processing conditions and of the direction in which it was measured.

There was no significant effect of the CB-type.

Surface resistivity The surface resistivity, ρ_s, was measured at the surface and 0.2, 0.5, and 1.7 mm from the surface, after successively microtoming away 30 μm thick slices. The distance of 1.7 mm relates to the centre of the sample, taken from the middle part of the test bars. The measuring area was 10×2 mm.

The results for the flow direction for samples with a normal orientation are shown in Fig. 6. They relate to LDPE and HDPE with 10% KBEC or 20% VXC, the surface resistivity being plotted vs. *f*. As found for ρ_B measured on microtomed slices in the previous section, ρ_s had its highest values at the surface. Reducing the thickness by microtoming gave consistently lower ρ_s-values, the minimum being reached at the centre. The difference between the

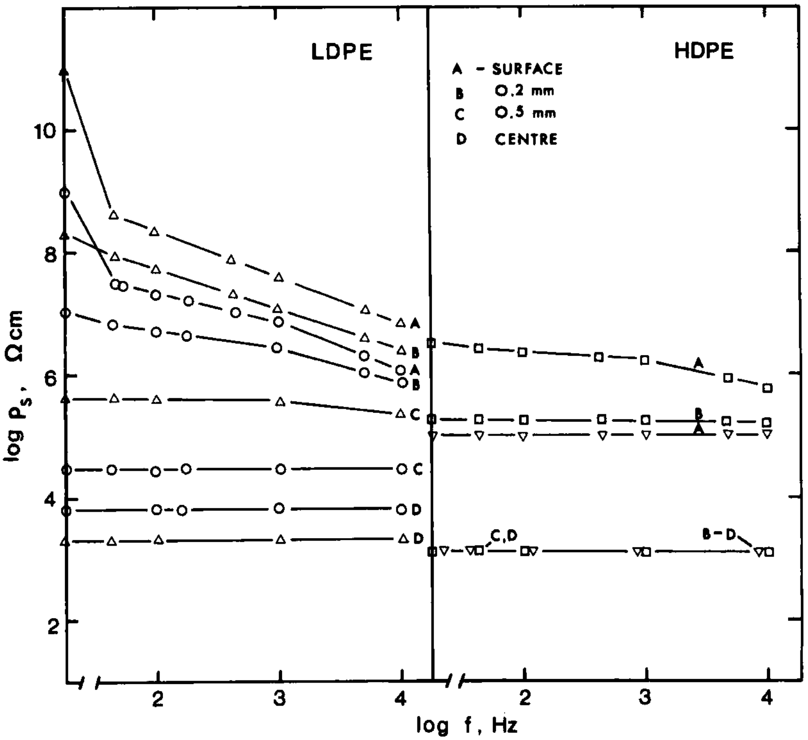

FIGURE 6 Frequency dependence of the surface resistivity, ρ_s, in the flow (x-) direction at the surface, and 0.2 mm, 0.5 mm and 1.7 mm (centre) from the surface. Normal orientation. Symbols as in Figure 2 (LDPE, left; HDPE, right).

centre and the surface was substantial (7 decades for LDPE/KBEC).

The highest ρ_s-values at the surface were obtained with LDPE/KBEC. For HDPE, the difference in ρ_s between the surface and the centre was substantially lower, while there was no significant difference between the two CB-types. Furthermore, HDPE had the same ρ_s-value at the centre and at 0.2 and 0.5 mm from the surface. For the LDPE-compunds the difference in ρ_s between these layers amounted to several decades. Unlike the case at the surface the LDPE/VXC-compound had a slightly higher ρ_s-value at the centre than did the KBEC-based compound. The LD- and HDPE-based compounds did not differ much at the centre, the differences being smaller than 1 decade for all four compounds.

The surface resistivity in the core region was approximately the same as that measured on isotropic samples prepared by compression moulding using the same moulding temperature as during the mixing (200°C; heating without pressure for 15 min, 30 MPa for 2 min, cooling 5°C/min). Similarly, there was no frequency dependence in the latter case.

Not shown in Fig. 6 are the ρ_s-values in the y-direction. For LDPE, the y-direction value of ρ_s at the surface was 2–5 times higher than the x-value. At the centre, the two values were about equal. For HDPE, the y-value was *c.* 10 times higher at the surface; about 0.1 mm beneath the surface and toward the centre, the two values became practically equal.

The frequency dependence of ρ_s was pronounced at high ρ_s-levels (above c. $10^6\,\Omega$cm), ρ_s decreasing with increasing f.

The dependence of ρ_s (DC) in the flow direction on the distance from the surface is clearly seen in Fig. 7. There was a pronounced difference between LD and HDPE, the ρ_s-value rapidly attaining a constant value at the centre of the sample. For LDPE, this decrease was more gradual, although the values at the centre were close to those obtained with HDPE. This was even more pronounced for the highly oriented samples; in this case, the ρ_s-values at the centre for LDPE were significantly higher than for HDPE.

With LDPE having a normal orientation, there is an inflexion in the ρ_s-distance from the surface curves, lying approximately between the shear and packing shear zones as evaluated from shrinkage measurements (Fig. 2).

With regard to the influence of the CB-type, KBEC-containing

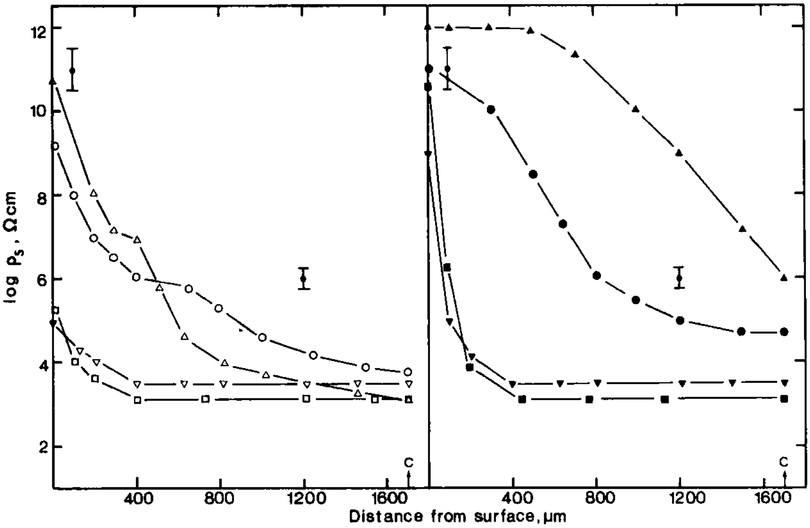

FIGURE 7 Surface resistivity (DC-value) in the flow direction vs. distance from the surface for samples having normal orientation (left) and high orientation (right). Symbols as in Figure 2.

LDPE showed the slowest variation of the ρ_s-value with the distance from the surface when the sample with the higher orientation was considered. For the normally oriented sample, the difference between KBEC and VXC was less significant. Similar trends, although less pronounced, were noted with HDPE.

On the whole, the shrinkage data of Fig. 2 did not provide a useful guidance in interpreting the ρ_s-data.

The data of Fig. 8 show the ρ_s (DC) vs. distance from the surface profiles for the x- and y-directions of LD and HDPE/KBEC. The y-direction value of ρ_s is slightly higher at the surface, the difference decreasing towards the centre. With VXC, similar results were obtained. The samples had a normal orientation.

The frequency dependence of ρ_s in the flow direction of the samples with the higher orientation is shown in Fig. 9. It may be noted that the increase in overall orientation resulted in an amplification of the effects recorded with normally oriented samples (Fig. 6). This applies, for instance, to the effect of the CB-type, the VXC-grade producing a significantly higher ρ_s-level at the centre.

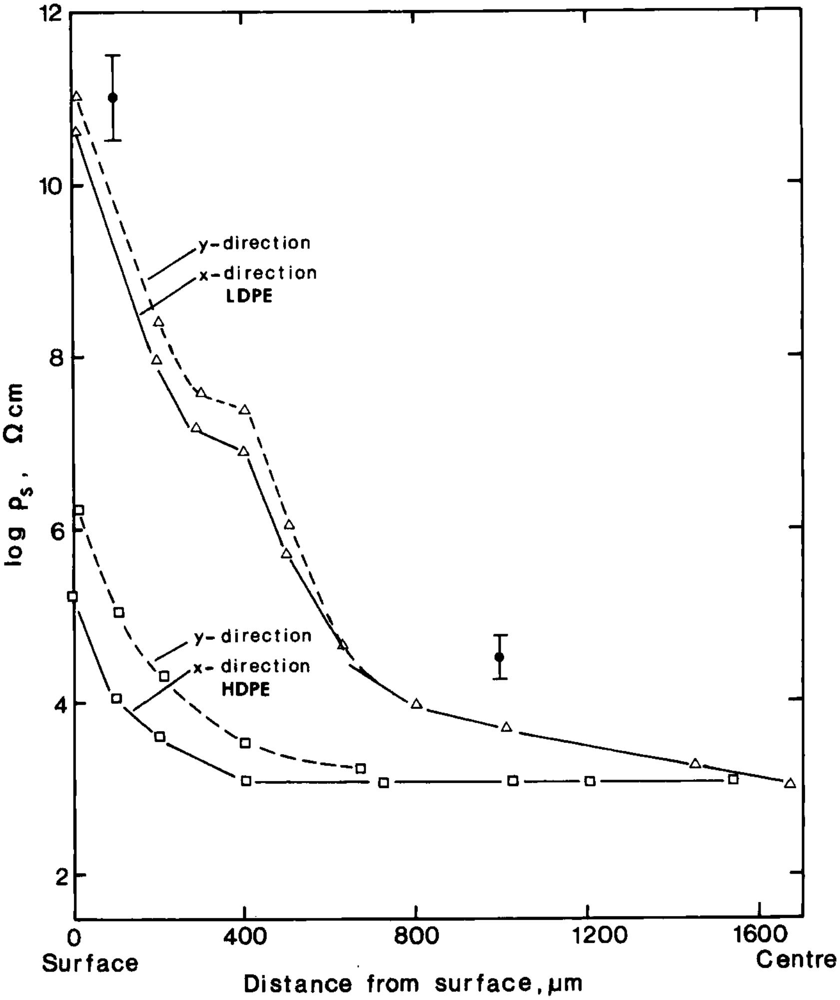

FIGURE 8 Surface resistivity (DC-value) in the x- and y-direction (see Figure 3) vs. distance from the surface. LDPE and HDPE with 10% KBEC, normal orientation. Symbols as in Figure 2.

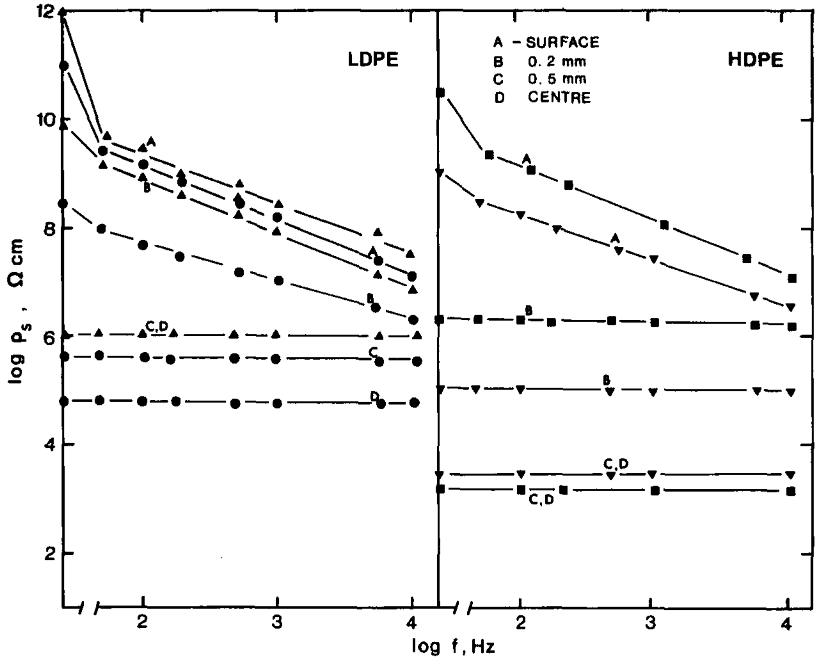

FIGURE 9 Frequency dependence of ρ_s in the flow direction at varying distance from the surface. High orientation. Symbols as in Figure 2 (LDPE, left; HDPE, right).

This was true of both LD and HDPE. At the surface, the opposite was true, KBEC giving the highest resistivities. Again, below *c.* 10^6 Ωcm there was no variation of ρ_s with frequency.

Surface resistivity vs. orientation Attempts to correlate resistivity data with the degree of orientation (shrinkage) did not produce any simple correlation. As the ρ_s-values showed an acceptable scatter, they were plotted vs. the corrected x-shrinkage of microtomed slices taken at a depth corresponding to that at which ρ_s was measured after gradually cutting away such slices from the sample. The result of this comparison, relating to the flow direction, is shown in Fig. 10. As the maxima in the shrinkage profiles (cf. Fig. 2) are not reflected in the ρ_s-profiles, the curves shown in Fig. 10 exhibit a rather erratic course. Qualitatively, there was a trend towards increasing ρ_s with orientation. For LDPE, this increase was rather gradual, while for HDPE the ρ_s-value remained constant until a critical orientation was reached, whereafter it showed a very steep ascent. This was, however, only true of the samples with the higher orientation; the normally oriented sample behaved similarly to LDPE, although the changes in ρ_s and orientation were much smaller.

The data of Fig. 10 show again that the resistivity at the surface, because of a higher orientation, was in general higher. Another factor possibly responsible for this behaviour is the difference in crystal morphology and overall crystallinity between the surface and the core. DTA measurement on the samples used showed a lower crystallinity at the surface. This has also been confirmed by others.[48]

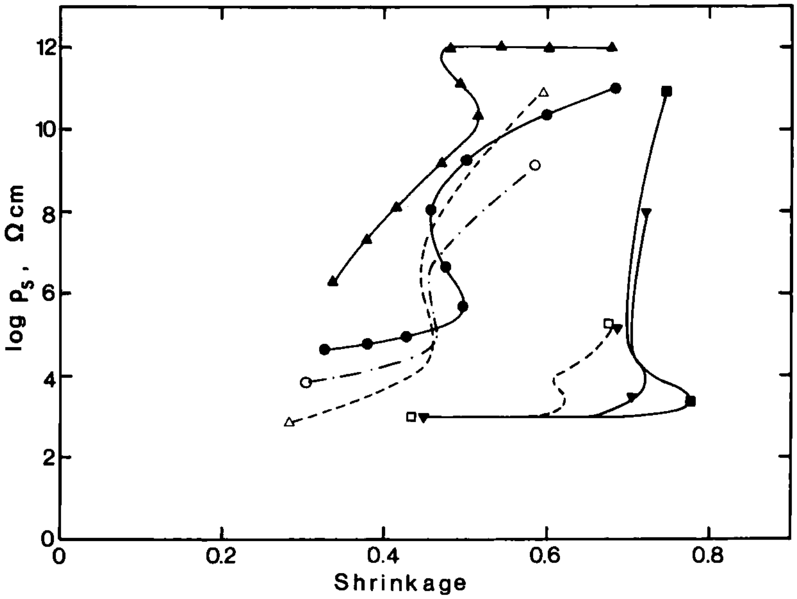

FIGURE 10 Surface resistivity (DC) vs. shrinkage in flow direction. Symbols as in Figure 2.

Final remarks

Injection-moulded parts normally show a layered structure. The difference between these layers relates mainly to structural features, as orientation of the chains or crystallites, crystallinity, and spherulite size.[49,50] Extensional flow and momentaneous solidification upon the contact with the mould cavity determine the structure of the surface layer, while a high shear rate is the structure-governing factor in the shear zone. The core, being the slowest solidifying region, is relatively unaffected by processing.

The structural features of the various layers appear to be reflected in the conductivity values and their anisotropy. When interpreting the results, however, one should keep in mind the complicated character of a composite of the type used here. Apparently, the conductivity is determined by a network of CB particles, the structure of which strongly depends on the pre-treatment of the material, the nature of the CB-grade used, and on the structure of the polymer within which this network is formed. The large differences in conductivity observed between the different layers of the moulded samples or between samples moulded under different conditions can be understood only when assuming that the mechanism underlying these effects is the disruption of the CB-network.

The elusive nature of such a process, implying changes in the connectivity of the network, highly reduces the prospects for a physical description of the effects observed. In this respect, the network behaves differently from the matrix, the state of which is described by suitable orientation measures. In addition, the CB-concentrations used here produce networks in the critical concentration range, where even small flow deformations, like small changes in the CB-content, may produce an appreciable variation in conductivity.

Qualitatively, the findings of this paper show that the resistivity of CB-filled PE increases with the degree of orientation. In the surface and shear zones of the moulded samples, the orientation, and thus the disrupted state of the CB-network are frozen-in. The core, on the other hand, is allowed to relax for a longer time, a process resulting in a recovery of the network and a restoration of the conductivity parameters characteristic of the undeformed state.

Apart from the pronounced dependence of the conductivity on the state of flow and deformation frozen into different regions of the sample, the frequency dependence of the conductivity represents another interesting feature of the results obtained.[51,52] This dependence increases with the resistivity level, i.e. with the degree of disruption of the conducting network. Consequently, it is most pronounced in the surface and shear zones, while it disappears in the core. Apparently, it is closely related to the conduction mechanisms. As will be shown in a forthcoming paper, the frequency dependence is accompanied by a non-ohmic behaviour. Annealed samples, or samples taken from the core region of the moulded test bars, show an ohmic conductivity not depending on frequency. Furthermore, it will be shown that the intensity of the PTC-effect is significantly enhanced by increasing anisotropy.

Acknowledgement

The authors wish to express their thanks to the Swedish Board for Technical Development for supporting this project financially. Thanks are also due to Dan Jönsson, M.Sc., for skilful experimental assistance.

References

1. A. Voet, *Rubber Chem. Technol.*, **54,** 42 (1981).
2. J. Meyer, *Polym. Eng. Sci.*, **13,** 462 (1973).
3. C. Klason and J. Kubát, *J. Appl. Polym. Sci.*, **19,** 831 (1975).
4. F. Bueche, *J. Appl. Phys.*, **44,** 532 (1973).
5. K. Ohe and Y. Haito, *Jap. J. Appl. Phys.*, **10,** 99 (1971).
6. U.S. 4,177,376.
7. C. Rajagopal and M. Satyam, *J. Appl. Phys.*, **49,** 5536 (1978).
8. A. Sternfield, *Mod. Plastics Int.*, **12: 7,** 48 (1982).
9. Anon., *Electronics,* Jan. 13, 28 (1981).
10. M. Narkis, A. Ram and F. Flasher, *Polym. Eng. Sci.*, **18,** 649 (1978).
11. *iidem, J. Appl. Polym. Sci.*, **22,** 1163 (1978).
12. L. Nicodemo, L. Nicolais, G. Romeo and E. Scafora, *Polym. Eng. Sci.*, **18,** 293 (1978).
13. S. K. Bhattacharyya, S. Basu and S. K. De, *J. Appl. Polym. Sci.*, **25,** 111 (1980).
14. F. F. T. de Araujo and H. M. Rosenberg, *J. Phys. D: Appl. Phys.*, **9,** 1025 (1976).
15. S. Littlewood and B. F. N. Briggs, *ibid.*, **11,** 1457 (1978).
16. M. Narkis, A. Ram and Z. Stein, *Polym. Eng. Sci.*, **21,** 1049 (1981).
17. iidem, *J. Appl. Polym. Sci.*, **25,** 1515 (1980).
18. J. Meyer, *Polym. Eng. Sci.*, **14,** 706 (1974).
19. A. I. Medalia, *Rubber Chem. Technol.*, **51,** 437 (1978).
20. A. Voet, A. K. Sircar and T. J. Mullens, *ibid.*, **42,** 874 (1969).
21. W. F. Verhelst, K. G. Wolthius, A. Voet, P. Ehrburger and J. B. Donnet, *ibid.*, **50,** 735 (1977).

22. R. Chasset and P. Thirion, *Rev. Gén. Caout.*, **38,** 1455 (1961).
23. A. Voet, F. R. Cook and A. K. Sircar, *Rubber Chem. Technol.*, **44,** 175 (1971).
24. A. K. Sircar, A. Voet and F. R. Cook, *ibid.*, **44,** 185 (1971).
25. P. E. Wack, R. L. Anthony and E. Guth, *J. Appl. Phys.*, **18,** 456 (1947).
26. S. de Meij, *Kaut. Gummi*, **11: 5,** 138 (1958).
27. R. H. Norman, *Eur. Rubber J.*, **163: 9,** 20 (1981).
28. A. K. Sircar and T. G. Lamond, *Rubber Chem. Technol.*, **51,** 126 (1978).
29. R. J. Kirschbaum, Tech. Report RG-128, Cabot, (1978).
30. A. Voet and J. C. Morawski, *Rubber Chem. Technol.*, **47,** 765 (1974).
31. A. R. Payne, *J. Appl. Polym. Sci.*, **9,** 1073 (1965).
32. K. Ziermann, *Kaut. Gummi Kunstst.*, **21: 4,** 159 (1968).
33. B. Brokenbrow, D. Sims and A. L. Stokoe, *Rubber, J.*, Dec., 51 (1969).
34. D. L. Walker, *Rubber Chem. Technol.*, **28,** 519 (1955).
35. S. K. Bhattacharyya, *Polymer*, **20,** 1166 (1979).
36. D. R. Poole, *Plastics Eng.*, **34: 6,** 25 (1978).
37. A. M. Hermann, S. P. S. Yen, A. Rembaum and R. F. Landel, *Polym. Letters*, **9,** 627 (1971).
38. R. Gilg, *Kunststoffberater*, **22: 6,** 312 (1977).
39. V. E. Gul, R. M. Kessenikh, N. E. Molodykh and L. V. Kolesnikov, *Plast. Massy*, No 4, 30 (1972).
40. A. D. Ageev, S. A. Andronava and G. V. Sagalaev, *Int. Polym. Sci. Technol.*, **4: 9,** 64 (1977).
41. W. J. Green, S. Verne and D. E. Evans, Brit. 828,233 (1957).
42. P. C. Woodland and E. E. Ziegler, *Mod. Plast.*, **28: 9,** 95 (1951).
43. B. Wargotz, *Trans. J. Plast. Inst.*, **35,** 783 (1967).
44. R. H. Norman, *Conductive Rubber; its Production, Application and Test Methods* (Maclaren, London, 1957).
45. G. Menges and G. Wübken, *Plastverarbeiter*, **23,** 41 (1973).
46. G. Wübken, *ibid.*, **26,** 17 (1975).
47. J. Kubát, J.-A. Månson and H.-E. Strömvall, *J. Mater. Sci.*, **17,** 915 (1982).
48. F. H. Moy and M. R. Kamal, *Polym. Eng. Sci.*, **20,** 957 (1980).
49. M. R. Kantz, H. D. Newman and F. H. Stigale, *J. Appl. Polym. Sci.*, **16,** 1249 (1972).
50. Z. Tadmor, *ibid.*, **18,** 1753 (1974).
51. H. H. Hassan and M. K. El-Mansy, *Gummi, Asbest. Kunstst.*, **5,** 204 (1983).
52. K. T. Chung, A. Sabo and A. P. Pica, *J. Appl. Phys.*, **53,** 6867 (1982).